
Magnesium isotopic composition of the deep continental crust

Wei Yang^{1,*}, Fang-Zhen Teng^{2,*}, Wang-Ye Li³, Sheng-Ao Liu⁴, Shan Ke⁴, Yong-Sheng Liu⁵, Hong-Fu Zhang⁶, Shan Gao⁵

¹Key Laboratory of Earth and Planetary Physics, Institute of Geology and Geophysics, Chinese Academy of Sciences, Beijing 100029, China

²Isotope Laboratory, Department of Earth and Space Sciences, University of Washington, Seattle, WA 98195, USA

³CAS Key Laboratory of Crust–Mantle Materials and Environments, School of Earth and Space Sciences, University of Science and Technology of China, Hefei 230026, China

⁴State Key Laboratory of Geological Processes and Mineral Resources, China University of Geosciences, Beijing 100083, China

⁵Faculty of Earth Sciences, China University of Geosciences, Wuhan 430074, China

⁶State Key Laboratory of Lithospheric Evolution, Institute of Geology and Geophysics, Chinese Academy of Sciences, Beijing 10029, China

Revised Version 1

April 22 2015

* Corresponding author, E-mail address: yangw@mail.iggcas.ac.cn;
fteng@u.washington.edu

1 **Abstract:**

2 To constrain the behavior of Mg isotopes during deep crustal processes and the
3 Mg isotopic composition of the middle and lower continental crust, 30 composite
4 samples from high-grade metamorphic terranes and 18 granulite xenoliths were
5 investigated. The composites derive from 8 different high-grade metamorphic terranes
6 in the two largest Archean cratons of China, including 13 TTG gneisses, 5
7 amphibolites, 4 felsic, 4 intermediate and 4 mafic granulites. They have variable bulk
8 compositions with SiO₂ ranging from 45.7 to 72.5%, representative of the middle
9 crust beneath eastern China. The $\delta^{26}\text{Mg}$ values of these samples vary from -0.40 to
10 +0.12‰, reflecting heterogeneity of their protoliths, which could involve upper
11 crustal sediments. The granulite xenoliths from the Cenozoic Hannuoba basalts also
12 have a diversity of compositions with MgO ranging from 2.95 to 20.2%. These
13 xenoliths equilibrated under high temperatures of 800–950 °C, corresponding to
14 depths of the lower continental crust (> 30 km). They yield a large $\delta^{26}\text{Mg}$ variation of
15 -0.76 ~ -0.24‰. The light Mg isotopic compositions likely result from interactions
16 with isotopically light metamorphic fluids, probably carbonate fluids. Together with
17 previously reported data, the average $\delta^{26}\text{Mg}$ of the middle and lower continental
18 crusts is estimated to be $-0.21 \pm 0.07\text{‰}$ and $-0.26 \pm 0.06\text{‰}$, respectively. The bulk
19 continental crust is estimated to have an average $\delta^{26}\text{Mg}$ of $-0.24 \pm 0.07\text{‰}$, which is
20 similar to the average of the mantle. The large Mg isotopic variation in the continental
21 crust reflects the combination of several processes, such as continental weathering,
22 involvement of supracrustal materials in the deep crust, and fluid metasomatism.

23

24 **Keywords:** magnesium isotope, deep continental crust, high-grade metamorphic
25 terrane, granulite xenolith

26

27 **Introduction**

28 Magnesium is a fluid-mobile, major element, and has three isotopes of ^{24}Mg ,
29 ^{25}Mg and ^{26}Mg . Magnesium isotope fractionation is limited during high temperature
30 processes (Teng et al., 2007; 2010a; Handler et al., 2009; Yang et al., 2009; Bourdon
31 et al., 2010; Liu et al., 2010), but is significant during low temperature processes
32 (Young and Galy, 2004; Tipper et al., 2006a; 2006b; 2010; Pogge von Strandmann et
33 al., 2008a; 2008b; Li et al., 2010; Teng et al., 2010b; Huang et al., 2012; Liu et al.,
34 2014). The mantle, upper continental crust and the hydrosphere have distinct Mg
35 isotopic compositions. The mantle is nearly homogeneous with $\delta^{26}\text{Mg}$ values ranging
36 from -0.48 to -0.06 ‰ (Teng et al., 2007; 2010a; Handler et al., 2009; Yang et al.,
37 2009; Bourdon et al., 2010; Dauphas et al., 2010; Pogge von Strandmann et al., 2011;
38 Xiao et al., 2013), whereas the upper continental crust is highly heterogeneous ($\delta^{26}\text{Mg}$
39 = -1.64 ~ +0.92‰) and on average heavier than the mantle (Shen et al., 2009; Li et al.,
40 2010; Liu et al., 2010; Huang et al., 2013a; Teng et al., 2013). The hydrosphere has a
41 very light Mg isotopic composition, as represented by seawater ($\delta^{26}\text{Mg} = -0.83 \pm$
42 0.09‰ , 2SD) (Foster et al., 2010; Ling et al., 2011 and references therein) and the
43 flux weighted average of major rivers ($\delta^{26}\text{Mg} = -1.09\text{‰}$) (Tipper et al., 2006b). These
44 Mg isotopic characteristics are considered to result from continental weathering,
45 during which light Mg isotopes are preferentially partitioned into the hydrosphere,
46 causing a shift in the weathered residues toward a heavier isotopic composition
47 (Pogge von Strandmann et al., 2008b; Teng et al., 2010b; Tipper et al., 2010; Huang et
48 al., 2012; Liu et al., 2014).

49 To better constrain the interaction between the crust and the hydrosphere, Mg
50 isotopic composition of the middle and lower continental crustal materials should also
51 be investigated since they contain large proportions of Mg in the crust. However, thus
52 far, only one study on this issue has been reported. Teng et al. (2013) investigated two
53 well-characterized suites of lower-crustal granulite xenoliths from the Chudleigh and
54 McBride volcanic provinces, North Queensland, Australia. The McBride granulites

55 display a very large variation in $\delta^{26}\text{Mg}$ values from -0.72 to +0.19‰, which was
56 considered to reflect both source heterogeneity and metamorphic enrichment of garnet.
57 Nonetheless, the Mg isotopic composition of the middle continental crust is still
58 unknown since granulite xenoliths are generally considered to be representative of the
59 lower crust (Rudnick and Gao, 2003). In addition, the $\delta^{26}\text{Mg}$ variation (-0.72 to
60 +0.19‰) observed in the McBride lower crustal granulites is quite large. Whether it is
61 a special case or a common phenomenon in the lower crust requires further research.

62 To constrain the behavior of Mg isotopes during deep crustal processes and the
63 Mg isotopic compositions of the middle and lower continental crusts, two suits of
64 samples from China have been investigated. One is a set of high-grade metamorphic
65 rocks from Archean terranes, and the other are granulite xenoliths from Damaping,
66 Hannuoba. Both suites have been systematically studied and are considered as
67 representative samples for the middle and lower continental crusts of eastern China
68 (Gao et al., 1998a; Liu et al., 2001; 2004; Teng et al., 2008). Our results reveal a large
69 Mg isotopic variation in the deep continental crust, which likely results from the
70 combination of several processes, such as continental weathering, involvement of
71 supracrustal materials in the deep crust, and fluid metasomatism. Nonetheless, the
72 bulk continental crust on average still has a mantle-like Mg isotopic composition.

73

74 **Samples and geological background**

75 The deep continental crust can be divided into two layers based on seismological
76 studies: the middle crust and the lower crust (Rudnick and Fountain, 1995). Two types
77 of samples can be used to determine the composition of the deep continental crust:
78 high-grade metamorphic terranes and lower crustal xenoliths. The former is often
79 considered to be representative of the middle crust (Bohlen and Mezger, 1989) and
80 the latter to be representative of the lower crust (Rudnick and Gao, 2003). Thirty
81 samples from the high-grade metamorphic terrane and 18 granulite xenoliths from
82 Eastern China are studied here. The geological background, sample description, major

83 and trace-element abundances and Sr, Nd, Pb and Li isotopic compositions of the
84 studied samples have been previously reported (Gao et al., 1998a; Liu et al., 2001;
85 2004; Teng et al., 2008). Only a brief summary is given below.

86

87 **High-grade metamorphic rocks from Archean terranes**

88 The samples were collected from 8 different high-grade metamorphic terranes in
89 the two largest Archean cratons of China (Fig. 1). The Kongling amphibolite-
90 granulite-facies terrane is from the Yangtze Craton, and the other 7 terranes are from
91 the North China craton, including Wutai and Dengfeng amphibolite-facies terranes,
92 Fuping, Hengshan and Taihua amphibolite-granulite-facies terranes, Jinning and
93 Wulashan granulite-facies terranes (Gao et al., 1999; Qiu et al., 2000). The samples,
94 including 13 TTG gneisses, 5 amphibolites, 4 felsic, 4 intermediate and 4 mafic
95 granulites, are composites that were produced by mixing equal amounts of individual
96 rock samples (n=1 to 15) having the same age and lithology from the same tectonic
97 unit. Sm-Nd and zircon U-Pb dating of these samples yielded 3.3 – 2.5 Ga (Gao et al.,
98 1998a). The individual rock samples were collected along road cuts, riverbanks, or
99 mountain valleys and are very fresh, as indicated by petrographic studies (Gao et al.,
100 1996; 1998a; 1999; Qiu et al., 2000). These composites are thus considered to be
101 representative of most Archean units exposed in eastern China.

102 The bulk compositions of these composites vary from mafic to felsic, with SiO₂
103 ranging from 45.7 to 72.5% and MgO from 0.4 to 7.7% (Fig. 2a). They are considered
104 to be representative of the middle crust beneath eastern China (Gao et al., 1998a;
105 1998b). They have relatively restricted Li isotopic composition with $\delta^7\text{Li}$ ranging
106 from +1.7 to +7.5‰ (Teng et al., 2008) (Fig. 2b).

107

108 **Granulite xenoliths from Damaping, Hannuoba, China**

109 The lower crustal xenoliths were collected from the Cenozoic Hannuoba basalts
110 (Zhang et al., 2013), which is situated in the central orogenic belt of the North China

111 Craton (Fig. 1). These xenoliths have a diversity of compositions, with SiO₂ ranging
112 from 44.2 to 60.3% and MgO from 2.95 to 20.2% (Gao et al., 2000; Chen et al., 2001;
113 Liu et al., 2001; 2004; Zhou et al., 2002). They are 4 to 20 cm in diameter and range
114 in composition from pyroxenite, plagioclase-rich mafic granulite to intermediate
115 granulite. All these xenoliths equilibrated under high temperatures (800 – 950 °C),
116 corresponding to depths greater than 30 km (Chen et al., 2001; Liu et al., 2003) (Fig.
117 3). U-Pb zircon chronology on these granulite xenoliths indicates that basaltic magma
118 intruded Precambrian lower crust at ~160–140 Ma and induced subsequent granulite-
119 facies metamorphism (Liu et al., 2004).

120 The samples can be divided into two groups based on MgO contents: high Mg
121 xenoliths and low Mg xenoliths. The high Mg xenoliths include pyroxenites, two-
122 pyroxene mafic granulites and garnet-bearing mafic granulites, with MgO ranging
123 from 12.4 to 20.2%, while the low Mg xenoliths include plagioclase-rich mafic
124 granulites and intermediate granulites, with MgO ranging from 2.95 to 6.97% (Fig.
125 2a). Both types have variable Li isotopic compositions, with δ⁷Li of -9.6 ~ +4.3‰ and
126 -5.1 ~ +13.8‰, respectively (Teng et al., 2008) (Fig. 2b). Such large variations of Li
127 isotopic compositions were considered to mainly result from source heterogeneity
128 (Teng et al., 2008). These xenoliths also show very large variations in Sr (⁸⁷Sr/⁸⁶Sr =
129 0.707 to 0.723), Nd (ε_{Nd} = -28.0 to -11.3) and Pb isotopic compositions (²⁰⁶Pb/²⁰⁴Pb =
130 16.16 to 17.91), probably reflecting mixing between preexisting Precambrian deep
131 crust with the underplated basaltic magmas (Liu et al., 2001; 2004).

132

133 **Analytical methods**

134 Magnesium isotopic analyses were performed at the Isotope Laboratory of the
135 University of Arkansas, Fayetteville, following the established procedures (Teng et al.,
136 2007; 2010a; Li et al., 2010; Yang et al., 2009; Teng and Yang, 2014). Only a brief
137 description is given below.

138 All chemical procedures were carried out in a clean laboratory environment.

139 Depending on Mg concentration, one to 25 mg of sample powder was weighted in
140 Savillex screw-top beakers in order to have > 50 μg Mg in the solution. The sample
141 powder was dissolved in a mixture of concentrated HF-HNO₃-HCl solution.
142 Separation of Mg was achieved by cation exchange chromatography with Bio-Rad
143 200-400 mesh AG50W-X8 resin in 1N HNO₃ media following the established
144 procedures (Teng et al., 2007; 2010a; Yang et al., 2009; Li et al., 2010). Magnesium
145 isotopic compositions were analyzed by the standard bracketing method using a Nu
146 Plasma MC-ICP-MS (Multi-Collector Inductively Coupled Plasma Mass
147 Spectrometry) at the University of Arkansas (Teng and Yang, 2014). Magnesium
148 isotope data are reported in standard δ -notation relative to DSM3: $\delta^{26}\text{Mg} =$
149 $[(\delta^{26}\text{Mg}/^{24}\text{Mg})_{\text{sample}} / (\delta^{26}\text{Mg}/^{24}\text{Mg})_{\text{DSM3}} - 1] \times 1000$. $\Delta^{25}\text{Mg}' = \delta^{25}\text{Mg}' - 0.521 \times \delta^{26}\text{Mg}'$,
150 where $\delta^{25, 26}\text{Mg}' = 1000 \times \ln[(\delta^{25, 26}\text{Mg} + 1000)/1000]$ (Young and Galy, 2004).

151 The internal precision of the measured $^{26}\text{Mg}/^{24}\text{Mg}$ ratio based on ≥ 4 repeat runs
152 of same sample solution during a single analytical session is $< \pm 0.07\text{‰}$ (Teng et al.,
153 2010a). Six replicate analyses of olivine KH-1 (Kilbourne Hole) yielded $\delta^{26}\text{Mg}$ values
154 of $-0.27 \pm 0.05\text{‰}$, which is in agreement with that reported by Teng et al. (2015)
155 ($\delta^{26}\text{Mg} = -0.27 \pm 0.07\text{‰}$; 2SD, n=16). The external precision, as shown by replicate
156 analyses of synthetic solution, mineral and rock standards, was $\pm 0.06\text{‰}$ for $\delta^{25}\text{Mg}$ and
157 $\pm 0.07\text{‰}$ for $\delta^{26}\text{Mg}$ (2SD) (Teng et al., 2010a; 2015).

158

159 **Results**

160 Magnesium isotopic compositions of composite samples from high-grade
161 metamorphic terranes are listed in Table 1 and granulite xenoliths in Table 2, along
162 with their chemical compositions. In a plot of $\delta^{25}\text{Mg}'$ vs. $\delta^{26}\text{Mg}'$ (Fig. 4), all samples
163 fall along the terrestrial equilibrium mass fractionation curve, with a slope of 0.521
164 (Young and Galy, 2004), with $\Delta^{25}\text{Mg}'$ values $< \pm 0.04\text{‰}$ (Tables 1 and 2).

165 Overall, Mg isotopic compositions vary significantly, with $\delta^{26}\text{Mg}$ ranging from -
166 0.76 to $+0.12\text{‰}$ and $\delta^{25}\text{Mg}$ from -0.39 to $+0.06\text{‰}$ (Tables 1 and 2). This variation is

167 quite similar to that of the lower crustal granulite xenoliths from Chudleigh and
168 McBride, Australia, with $\delta^{26}\text{Mg}$ from -0.72 to +0.19‰ (Teng et al., 2013), and falls
169 within the range of the upper continental crust ($\delta^{26}\text{Mg} = -1.64 \sim +0.92\text{‰}$) (Li et al.,
170 2010; Liu et al., 2010; Huang et al., 2013a).

171 The samples from Archean high-grade metamorphic terranes have a large
172 variation in Mg isotopic composition (Fig. 5), with $\delta^{26}\text{Mg}$ ranging from -0.40 to +0.12‰
173 and an average of $-0.22 \pm 0.19\text{‰}$ (2SD, n=30). Two samples (14R110, $+0.12 \pm 0.06\text{‰}$
174 and D148, $-0.05 \pm 0.09\text{‰}$) have $\delta^{26}\text{Mg}$ values deviating the population of the others (-
175 0.40 \sim -0.15‰, Fig. 6a). Samples from different localities do not display systematical
176 variations (Fig. 6b).

177 The high and low Mg granulite xenoliths from Hannuoba exhibit quite distinct
178 Mg isotopic compositions (Fig. 5). The high Mg granulite xenoliths show a limited
179 variation of 0.11‰ in $\delta^{26}\text{Mg}$ value from -0.37 to -0.26‰. However, the low Mg
180 granulite xenoliths display an obviously lighter Mg isotopic composition, with large
181 variations in $\delta^{26}\text{Mg}$ ranging from -0.76 to -0.24‰. Such a light Mg isotopic
182 composition of low Mg granulite xenoliths is comparable with the McBride granulites,
183 which have $\delta^{26}\text{Mg}$ values of -0.72 to +0.19‰ (Teng et al., 2013).

184

185 Discussion

186 The high-grade metamorphic terranes and granulite xenoliths from eastern China,
187 which are considered to be representative of the middle and lower continental crust
188 (Gao et al., 1998a; Liu et al., 2001; 2004; Teng et al., 2008), display up to 0.9‰
189 variation in Mg isotopic composition. Based on studies of peridotites, oceanic basalts
190 and granites (Teng et al., 2007; 2010a; Handler et al., 2009; Yang et al., 2009;
191 Bourdon et al., 2010; Liu et al., 2010), no more than 0.07‰ Mg isotope fractionation
192 will occur during closed-system partial melting of the mantle and fractional
193 crystallization of basaltic or granitic magma. Therefore, the large variation in the Mg
194 isotopic composition of the deep crustal rocks must be due to source heterogeneity

195 and/or other processes. Below, we first evaluate each of these mechanisms for both
196 terrane and xenolith samples, and then estimate the average Mg composition of the
197 continental crust.

198

199 **Magnesium isotopic systematics of the Archean high-grade metamorphic**
200 **terranes from the eastern China**

201 The 30 samples from Archean high-grade metamorphic terranes yield a $\delta^{26}\text{Mg}$
202 variation ranging from -0.40 to +0.12‰, among which 28 samples fall within the
203 range of the mantle rocks (-0.48 to -0.06 ‰) (Teng et al., 2007; 2010a; Handler et al.,
204 2009; Yang et al., 2009; Bourdon et al., 2010; Dauphas et al., 2010; Bizzarro et al.,
205 2011; Pogge von Strandmann et al., 2011). These samples also have a mantle-like Li
206 isotopic composition with $\delta^7\text{Li}$ ranging from +1.7 to +7.5‰ (Teng et al., 2008). The
207 mantle-like Li and Mg isotopic compositions of the Archean high-grade metamorphic
208 terranes indicate that they inherited Li and Mg isotopic compositions of their
209 protoliths, which have not been modified by subsequent processes.

210 The other two samples (14R110 and D148) yield relatively high $\delta^{26}\text{Mg}$ values of
211 $+0.12 \pm 0.06\text{‰}$ and $-0.05 \pm 0.09\text{‰}$, respectively (Fig. 5). Three potential mechanisms
212 could result in the heavy Mg isotopic compositions: (1) surface weathering; (2)
213 metamorphism; and/or (3) protolith heterogeneity.

214 Surface weathering can significantly modify Mg isotopic compositions of rocks
215 towards heavy values (Pogge von Strandmann et al., 2008a; Teng et al., 2010b; Huang
216 et al., 2012; Liu et al., 2014). However, the high-grade metamorphic samples studied
217 here were carefully collected and are very fresh as indicated by petrographic studies
218 (Gao et al., 1998a). Therefore, the effects of weathering are considered to be
219 negligible. This is also supported by the Li isotopic composition of these samples.
220 Surface weathering can significantly fractionate Li isotopes and result in large
221 variations in both Li isotopic composition and Li concentration in the weathered
222 products (Teng et al., 2004). However, all these high-grade metamorphic samples

223 have similar and mantle-like Li isotopic compositions (Teng et al., 2008).

224 The relatively heavy Mg isotopic composition of these two samples may thus
225 reflect either metamorphism or protolith heterogeneity. Most progressive
226 metamorphic reactions are accompanied by dehydration, leading to the depletion of
227 fluid-mobile elements in the high-grade metamorphic rocks (Rudnick et al., 1985).
228 Lithium and Mg both are fluid mobile. During dehydration, ^7Li and ^{24}Mg
229 preferentially enters fluids over most minerals, leading to lower $\delta^7\text{Li}$ and higher
230 $\delta^{26}\text{Mg}$ in rocks. The extent of isotope fractionation is determined by the fraction of Li
231 and Mg released from rocks into fluids and the fractionation factor ($\alpha_{\text{fluid-rock}}$).
232 Theoretically, this process may not affect Mg isotopic systematics. Since Mg contents
233 in the silicate rocks are at least 10-100 times higher than those in the fluid (Brenot et
234 al., 2008), Mg isotopic composition of rocks is expected to change little with such a
235 small loss of Mg. This was demonstrated by previous studies on eclogites, granulites
236 and metapelites (Li et al., 2011; 2014; Teng et al., 2013; Wang et al., 2014b). Though
237 significant (up to 3%) amount of fluid was lost during metamorphic dehydration,
238 eclogites, granulites and metapelites still have similar Mg isotopic composition to
239 their protoliths, suggesting limited Mg isotope fractionation during metamorphic
240 dehydration (Li et al., 2011; 2014; Teng et al., 2013; Wang et al., 2014b).

241 Therefore, the most likely mechanism for the heavy $\delta^{26}\text{Mg}$ values of these two
242 samples (14R110 and D148) is the involvement of upper crustal sediments in their
243 protoliths. Sedimentary rocks have highly heterogeneous and, in most cases, heavy
244 Mg isotopic compositions, with $\delta^{26}\text{Mg}$ ranging from -0.52 to +0.92‰ (Li et al., 2010).
245 These two samples also have evolved compositions with $\text{SiO}_2 = 70.84$ and 71.84% .
246 However, other samples (D139, D140, D142 and D143) with even higher SiO_2
247 contents ($72.03 - 72.54\%$) do not exhibit high $\delta^{26}\text{Mg}$ values ($-0.24 - -0.35\%$).
248 Possible explanation is that the sedimentary materials have a very large range of Mg
249 isotopic composition ($\delta^{26}\text{Mg} = -0.52$ to $+0.92\%$) and only a part of them has heavy
250 Mg isotopic composition ($\delta^{26}\text{Mg} > 0\%$). Nevertheless, the majority of the terrane

251 samples have a mantle-like Mg isotopic composition ($\delta^{26}\text{Mg} = -0.40$ to -0.15%), and
252 samples from different localities do not display systematic variation (Fig. 6b),
253 indicating that the Mg isotopic compositions of the middle crust beneath both the
254 North China craton and the South China craton are quite similar.

255

256 **Magnesium isotopic systematics of the Hannuoba granulite xenoliths from the**
257 **Eastern China**

258 The high and low Mg granulite xenoliths from Hannuoba exhibit quite distinct
259 Mg isotopic compositions (Fig. 5). The high Mg granulite xenoliths falls within the
260 mantle range ($\delta^{26}\text{Mg} = -0.48$ to -0.06) (Teng et al., 2007; 2010a; Handler et al., 2009;
261 Yang et al., 2009; Bourdon et al., 2010; Dauphas et al., 2010; Bizzarro et al., 2011;
262 Pogge von Strandmann et al., 2011; Xiao et al., 2013), indicating an inheritance of Mg
263 isotopic compositions of their protoliths, because their high MgO contents make it
264 difficult to modify by other processes.

265 However, the low Mg granulite xenoliths display an obviously lighter Mg
266 isotopic composition with large variations in $\delta^{26}\text{Mg}$ ranging from -0.76 to -0.24% .
267 Since Mg isotope fractionation during the progressive metamorphic reactions is
268 limited (Li et al., 2011; 2014; Teng et al., 2013; Wang et al., 2014b), the light Mg
269 isotopic composition of the Hannuoba granulite xenoliths may result from one or a
270 combination of the following processes: (1) unrepresentative sampling, (2) protolith
271 heterogeneity, (3) interaction with host magma, (4) interaction with fluid (fluid
272 metasomatism).

273 For small-size xenoliths with coarse-grained minerals, a mineralogically
274 unrepresentative sampling could result in bias in the Mg isotopic composition of the
275 whole rock (Teng et al., 2013). For example, garnet is isotopically lighter than
276 clinopyroxene in eclogite (Li et al., 2011; Wang et al., 2012; 2014a; 2014b), and its
277 preferential enrichment could result in light isotopic composition of the whole rock
278 (Teng et al., 2013). The McBride xenolith (83-162), which contains an overabundance

279 of metamorphic garnet, has a very low $\delta^{26}\text{Mg}$ value of -0.72‰ (Teng et al., 2013).
280 The light Mg isotopic composition of the low Mg granulite xenoliths in Hannuoba
281 could not result from unrepresentative sampling, because these samples are garnet
282 absent (Table 3). The only two garnet-bearing mafic granulites (DMP-08 and DMP-15)
283 are high Mg granulite xenoliths. They have low Ni/Ho (308 ~ 309) and Cr/Ho (438 ~
284 538) ratios (Fig. 7) relative to the other high Mg granulites, probably indicating
285 preferential sampling of garnet (Teng et al., 2013). However, their Ni/Ho and Cr/Ho
286 ratios are obviously higher than those of the two unrepresentative samples reported by
287 Teng et al. (2013), which have extremely low Ni/Ho (< 60) and Cr/Ho (< 60) ratios
288 (Fig. 7). In addition, their $\delta^{26}\text{Mg}$ values (-0.37‰ and -0.31‰) are still in the mantle
289 range. Thus, the unrepresentative sampling does not play a significant role in
290 controlling Mg isotopic variation in the Hannuoba xenoliths.

291 Another mechanism to generate the large Mg isotopic variation in the Hannuoba
292 granulite xenoliths is protolith heterogeneity. The high Mg and low Mg granulites
293 display differences not only in Mg isotopic composition, but also in Nd, Pb and Li
294 isotopic compositions (Fig. 8 and Fig. 9). The large variations in Nd and Pb isotopic
295 compositions are considered to reflect mixing between preexisting Precambrian deep
296 crust with the underplated basalts (Liu et al., 2001; 2004). In order to produce the
297 mixing trends observed in $\delta^{26}\text{Mg}$ vs. $^{206}\text{Pb}/^{204}\text{Pb}$ (Fig. 8a) and $\delta^{26}\text{Mg}$ vs. $\epsilon_{\text{Nd}}(t)$ plots
298 (Fig. 8b), the preexisting Precambrian deep crust with low $^{206}\text{Pb}/^{204}\text{Pb}$ and $\epsilon_{\text{Nd}}(t)$
299 should have a mantle-like Mg isotopic composition, whereas the underplated basalt
300 should have a light Mg isotopic composition ($\delta^{26}\text{Mg} < -0.76\text{‰}$). However, such a
301 light value ($< -0.76\text{‰}$) has not been observed in the Mesozoic and Cenozoic basalts
302 from the North China craton, which have $\delta^{26}\text{Mg}$ of $-0.60 \sim -0.42\text{‰}$ (Yang et al., 2012).
303 In addition, the low Mg concentrations (2.95 to 6.97%) of these samples indicate that
304 the involvement of underplated basalts, if any, is limited. Hence, the protolith
305 heterogeneity resulted from mixing with underplated basalts may not play a major
306 role in lowering the $\delta^{26}\text{Mg}$ value of the xenoliths, and additional processes are

307 required to produce the light Mg isotopic composition.

308 The third possibility to generate light Mg isotopic composition of the xenoliths is
309 through interactions with host magmas. During ascent to the Earth's surface, granulite
310 xenoliths and host magmas are generally not in thermal and chemical equilibrium.
311 This process can result in interaction between xenoliths and host magmas. To generate
312 a light Mg isotopic composition observed in the Hannuoba granulite xenoliths, the
313 host magma should have an even lighter Mg isotopic composition ($\delta^{26}\text{Mg} < -0.76\text{‰}$).
314 It also seems impossible that host magmas could have such light Mg isotopic
315 composition, thus, interaction with host magmas may also not play a major role in
316 lowering the $\delta^{26}\text{Mg}$ value of the xenoliths.

317 The most likely mechanism to produce such a light Mg isotopic composition in
318 the Hannuoba granulite xenoliths is rock-fluid interaction during metamorphism.
319 Since ^7Li and ^{24}Mg preferentially enters fluids, fluids could have light Mg isotopic
320 composition and heavy Li isotopic composition. Interaction with fluids should
321 generate a negative correlation between $\delta^7\text{Li}$ and $\delta^{26}\text{Mg}$ in rocks, which has been
322 observed in the Hannuoba granulite xenoliths (Fig.9). In addition, Mg isotopic
323 compositions correlate with Rb, Ba and H_2O contents (Fig. 10), suggesting that the
324 granulites have been interacted with metamorphic fluids to various extents. Although
325 dehydration process can not affect Mg isotopic systematics in silicate rocks (Li et al.,
326 2011; 2014; Teng et al., 2013; Wang et al., 2014b), fluid metasomatism probably can,
327 especially for low Mg rocks. This is because Mg loss during dehydration represents
328 only a very small portion of bulk Mg in silicate rocks (Li et al., 2011; 2014; Teng et
329 al., 2013; Wang et al., 2014b), however, Mg add-in during fluid metasomatism could
330 be very large especially in an open system. This is consistent with the observation that
331 the low Mg granulites were modified more significantly in Mg isotopic composition
332 than the high Mg granulites (Fig. 5). It is difficult to do a mass balance calculation of
333 the rock-fluid reaction, because there is no Mg concentration and isotopic data of deep
334 fluids reported. The seawater contains 0.12% (53000 $\mu\text{mol/L}$) Mg (Tipper et al.,

2006a) with a $\delta^{26}\text{Mg}$ value of $0.832 \pm 0.068\text{‰}$ (Ling et al., 2011). The river water displays large variations of $\delta^{26}\text{Mg}$ ($-2.08 \sim -0.05\text{‰}$) (Tipper et al., 2006a; 2006b; 2008). Deep fluids (especially carbonate fluids) can contain higher Mg than the seawater, e.g. fluid inclusions can have up to 9% Mg (McCaig et al., 2000). Assuming a pure carbonate fluid with ~10% of Mg and -2‰ of $\delta^{26}\text{Mg}$, a fluid/rock ratio of 0.05 is required to produce the light Mg isotopic composition in the Hannuoba granulite xenoliths. This metasomatism by carbonate fluids may lead to formation of carbonate minerals. However, no carbonate mineral is observed in the Hannuoba granulite xenolith. Possible mechanism is that under T-P condition of 1 Gpa and 800-950 °C, carbonate-bearing granulites will experience complete decarbonation (Fig. 3). The decomposition of carbonate mineral released CO_2 , but remained light Mg isotopes in the rocks.

To summarize, all of the above processes could potentially lower $\delta^{26}\text{Mg}$ values of granulite xenoliths to various extent. Nonetheless, the major mechanism to produce such a light Mg isotopic composition in the Hannuoba granulite xenoliths is rock-fluid interaction.

Magnesium isotopic composition of the deep and bulk continental crust

Magnesium content and isotopic compositions of the crustal samples are highly variable (Fig. 11), thus we estimate the average Mg isotopic composition of the middle and lower crusts from eastern China by using the concentration-weighted $\delta^{26}\text{Mg}$ for terrane and granulite samples, respectively. The $\delta^{26}\text{Mg}$ of the middle crust is estimated to be $-0.21 \pm 0.07\text{‰}$, which is slightly higher than the average $\delta^{26}\text{Mg}$ of the mantle ($-0.25 \pm 0.07\text{‰}$) (Teng et al., 2010a).

The weighted average $\delta^{26}\text{Mg}$ value of the lower continental crust underneath the Hannuoba, eastern China is estimated to be $-0.36 \pm 0.05\text{‰}$, which is significantly lighter than that of Chudleigh and McBride, Australia (-0.18‰) (Teng et al., 2013), indicating distinct Mg isotopic compositions of the lower crust in different continents. Nevertheless, based on all available data, the average $\delta^{26}\text{Mg}$ of the lower continental

363 crust is estimated to be $-0.26 \pm 0.06\%$.

364 The average $\delta^{26}\text{Mg}$ of the bulk continental crust is estimated to be $-0.24 \pm 0.07\%$
365 by combining the average $\delta^{26}\text{Mg}$ value and Mg concentration of the upper crust (-0.22
366 $\pm 0.10\%$, 2.48 wt %), middle crust ($-0.21 \pm 0.07\%$, 3.59 wt %), and lower crust ($-$
367 $0.26 \pm 0.06\%$, 7.24 wt %), with their respective weight proportions of 0.337: 0.347:
368 0.317 (Huang et al., 2013b; Teng et al., 2013). The overall Mg isotopic composition
369 of the continental crust is similar to the average $\delta^{26}\text{Mg}$ of the mantle ($-0.25 \pm 0.07\%$)
370 (Teng et al., 2010a). The large Mg isotopic variation in the continental crust results
371 from the combination of several processes, such as continental weathering,
372 involvement of supracrustal materials in the deep crust, and fluid metasomatism.
373 Because all these processes can only significantly modify Mg isotopic compositions
374 of rocks with low MgO contents and fractionate Mg isotopes in opponent ways, the
375 bulk continental crust still remains a mantle-like Mg isotopic composition.

376

377 **Implications**

378 Magnesium isotopic composition of the continental crust can provide not only
379 important constraints on the behavior of Mg isotopes during deep crustal processes,
380 but also necessary parameters for the global Mg isotopic mass-balance calculation.
381 Our studies of high-grade metamorphic terrane samples and the Hannuoba granulite
382 xenoliths from eastern China, as well as previous studies on granulite xenoliths from
383 Queensland, Australia (Teng et al., 2013), reveal large Mg isotopic variation in the
384 deep crust ($\delta^{26}\text{Mg} = -0.76 \sim +0.19\%$), indicating that light Mg isotopic composition
385 could be a common phenomenon in the lower continental crust. In addition, the deep
386 continental crust beneath the eastern China was previously considered to be
387 homogeneous in Mg isotopic composition because granites derived from partial
388 melting of the deep continental crust from this region have a very small Mg isotopic
389 variation with $\delta^{26}\text{Mg}$ ranging from -0.35 to -0.14% (Li et al., 2010; Liu et al., 2010).
390 Our study suggests that although partial melting and granite differentiation do not

391 fractionate Mg isotopes, these processes may homogenize Mg isotopic composition of
392 the source rocks, and thus erase the detail information of the deep continental crust.

393

394 **Acknowledgement**

395 We thank Yan Xiao, Shuijiong Wang, Fang Huang and Shuguang Li for
396 discussion. Constructive comments from two anonymous reviewers and efficient
397 handling from Paul Tomascak are greatly appreciated. This work was supported by
398 the National Science Foundation of China (Grants 41173012, 41230209, 41322022,
399 41221002, 41328004) and National Science Foundation (EAR-0838227, EAR-
400 1056713 and EAR1340160).

401 **Reference**

- 402 Bizzarro, M., Paton, C., Larsen, K., Schiller, M., Trinquier, A., and Ulfbeck, D. (2011)
403 High-precision Mg-isotope measurements of terrestrial and extraterrestrial
404 material by HR-MC-ICPMS-implications for the relative and absolute Mg-
405 isotope composition of the bulk silicate Earth. *Journal of Analytical Atomic*
406 *Spectrometry*, 26(3), 565-577.
- 407 Bohlen, S.R., and Mezger, K. (1989) Origin of granulite terranes and the formation of
408 the lowermost continental crust. *Science*, 244(4902), 326-329.
- 409 Bourdon, B., Tipper, E.T., Fitoussi, C., and Stracke, A. (2010) Chondritic Mg isotope
410 composition of the Earth. *Geochimica et Cosmochimica Acta*, 74(17), 5069-
411 5083.
- 412 Brenot, A., Cloquet, C., Vigier, N., Carignan, J., and France-Lanord, C. (2008)
413 Magnesium isotope systematics of the lithologically varied Moselle river basin,
414 France. *Geochimica et Cosmochimica Acta*, 72(20), 5070-5089.
- 415 Chen, S.H., O'Reilly, S.Y., Zhou, X.H., Griffin, W.L., Zhang, G.H., Sun, M., Feng,
416 J.L., and Zhang, M. (2001) Thermal and petrological structure of the lithosphere
417 beneath Hannuoba, Sino-Korean Craton, China: evidence from xenoliths. *Lithos*,
418 56(4), 267-301.
- 419 Dasgupta, R. (2013) Ingassing, Storage, and Outgassing of Terrestrial Carbon through
420 Geologic Time. *Reviews in Mineralogy and Geochemistry*, 75(1), 183-229.
- 421 Dauphas, N., Teng, F.-Z., and Arndt, N.T. (2010) Magnesium and iron isotopes in 2.7
422 Ga Alexo komatiites: Mantle signatures, no evidence for Soret diffusion, and
423 identification of diffusive transport in zoned olivine. *Geochimica et*
424 *Cosmochimica Acta*, 74(11), 3274-3291.
- 425 Foster, G., von Strandmann, P., and Rae, J. (2010) Boron and magnesium isotopic
426 composition of seawater. *Geochemistry Geophysics Geosystems*, 11(8), Q08015.
- 427 Gao, S., Kern, H., Liu, Y.-S., Jin, S.-Y., Popp, T., Jin, Z.-M., Feng, J.-L., Sun, M., and
428 Zhao, Z.-B. (2000) Measured and calculated seismic velocities and densities for
429 granulites from xenolith occurrences and adjacent exposed lower crustal
430 sections: A comparative study from the North China craton. *Journal of*
431 *Geophysical Research*, 105(B8), 18965-18976.
- 432 Gao, S., Ling, W., Qiu, Y., Lian, Z., Hartmann, G., and Simon, K. (1999) Contrasting
433 geochemical and Sm-Nd isotopic compositions of Archean metasediments from

-
- 434 the Kongling high-grade terrain of the Yangtze craton: evidence for cratonic
435 evolution and redistribution of REE during crustal anatexis. *Geochimica et*
436 *Cosmochimica Acta*, 63(13-14), 2071-2088.
- 437 Gao, S., Luo, T.C., Zhang, B.R., Zhang, H.F., Han, Y.W., Zhao, Z.D., and Hu, Y.K.
438 (1998a) Chemical composition of the continental crust as revealed by studies in
439 East China. *Geochimica et Cosmochimica Acta*, 62(11), 1959-1975.
- 440 Gao, S., Zhang, B.-R., Jin, Z.-M., Kern, H., Ting-Chuan, L., and Zhao, Z.-D. (1998b)
441 How mafic is the lower continental crust? *Earth and Planetary Science Letters*,
442 161(1-4), 101-117.
- 443 Gao, S., Zhang, B.-R., Wang, D.-P., Ouyang, J.-P., and Xie, Q.-L. (1996) Geochemical
444 evidence for the Proterozoic tectonic evolution of the Qinling Orogenic Belt and
445 its adjacent margins of the North China and Yangtze cratons. *Precambrian*
446 *Research*, 80(1-2), 23-48.
- 447 Handler, M.R., Baker, J.A., Schiller, M., Bennett, V.C., and Yaxley, G.M. (2009)
448 Magnesium stable isotope composition of Earth's upper mantle. *Earth and*
449 *Planetary Science Letters*, 282(1-4), 306-313.
- 450 Huang, K.-J., Teng, F.-Z., Elsenouy, A., Li, W.-Y., and Bao, Z.-Y. (2013a) Magnesium
451 isotopic variations in loess: Origins and implications. *Earth and Planetary*
452 *Science Letters*, 374, 60-70.
- 453 Huang, K.-J., Teng, F.-Z., Wei, G.-J., Ma, J.-L., and Bao, Z.-Y. (2012) Adsorption-
454 and desorption-controlled magnesium isotope fractionation during extreme
455 weathering of basalt in Hainan Island, China. *Earth and Planetary Science*
456 *Letters*, 359–360(0), 73-83.
- 457 Huang, Y., Chubakov, V., Mantovani, F., Rudnick, R.L., and McDonough, W.F.
458 (2013b) A reference Earth model for the heat-producing elements and associated
459 geoneutrino flux. *Geochemistry, Geophysics, Geosystems*, 14(6), 2003-2029.
- 460 Li, W.-Y., Teng, F.-Z., Wing, B.A., and Xiao, Y. (2014) Limited magnesium isotope
461 fractionation during metamorphic dehydration in metapelites from the Onawa
462 contact aureole, Maine. *Geochemistry, Geophysics, Geosystems*, 15(2), 408-415.
- 463 Li, W.-Y., Teng, F.-Z., Xiao, Y., and Huang, J. (2011) High-temperature inter-mineral
464 magnesium isotope fractionation in eclogite from the Dabie orogen, China. *Earth*
465 *and Planetary Science Letters*, 304(1-2), 224-230.
- 466 Li, W.Y., Teng, F.Z., Ke, S., Rudnick, R.L., Gao, S., Wu, F.Y., and Chappell, B.W.

-
- 467 (2010) Heterogeneous magnesium isotopic composition of the upper continental
468 crust. *Geochimica et Cosmochimica Acta*, 74(23), 6867-6884.
- 469 Ling, M.-X., Li, Y., Ding, X., Teng, F.-Z., Yang, X.-Y., Fan, W.-M., Xu, Y.-G., and
470 Sun, W. (2013) Destruction of the North China Craton Induced by Ridge
471 Subductions. *The Journal of Geology*, 121(2), 197-213.
- 472 Ling, M.-X., Sedaghatpour, F., Teng, F.-Z., Hays, P.D., Strauss, J., and Sun, W. (2011)
473 Homogeneous magnesium isotopic composition of seawater: an excellent
474 geostandard for Mg isotope analysis. *Rapid Communications in Mass
475 Spectrometry*, 25(19), 2828-2836.
- 476 Liu, S.-A., Teng, F.-Z., He, Y., Ke, S., and Li, S. (2010) Investigation of magnesium
477 isotope fractionation during granite differentiation: Implication for Mg isotopic
478 composition of the continental crust. *Earth and Planetary Science Letters*, 297(3-
479 4), 646-654.
- 480 Liu, X.-M., Teng, F.-Z., Rudnick, R.L., McDonough, W.F., and Cummings, M.L.
481 (2014) Massive magnesium depletion and isotope fractionation in weathered
482 basalts. *Geochimica et Cosmochimica Acta*, 135(0), 336-349.
- 483 Liu, Y.-S., Gao, S., Jin, S.-Y., Hu, S.-H., Sun, M., Zhao, Z.-B., and Feng, J.-L. (2001)
484 Geochemistry of lower crustal xenoliths from Neogene Hannuoba basalt, North
485 China craton: implications for petrogenesis and lower crustal composition.
486 *Geochimica et Cosmochimica Acta*, 65(15), 2589-2604.
- 487 Liu, Y., Gao, S., Liu, X., Chen, X., Zhang, W., and Wang, X. (2003) Thermodynamic
488 evolution of lithosphere of the North China craton: Records from lower crust and
489 upper mantle xenoliths from Hannuoba. *Chinese Science Bulletin*, 48(21), 2371-
490 2377.
- 491 Liu, Y.S., Gao, S., Yuan, H.L., Zhou, L., Liu, X.M., Wang, X.C., Hu, Z.C., and Wang,
492 L.S. (2004) U-Pb zircon ages and Nd, Sr, Pb isotopes of lower crustal xenoliths
493 from North China craton: insights on evolution of lower continental crust.
494 *Chemical Geology*, 211, 87-109.
- 495 McCaig, A.M., Tritlla, J., and Banks, D.A. (2000) Fluid mixing and recycling during
496 Pyrenean thrusting: evidence from fluid inclusion halogen ratios. *Geochimica et
497 Cosmochimica Acta*, 64(19), 3395-3412.
- 498 Nesbitt, H.W., and Young, G.M. (1982) Early Proterozoic climates and plate motions
499 inferred from major element chemistry of lutites. *Nature*, 299(5885), 715-717.

-
- 500 Pogge von Strandmann, P.A.E., Burton, K.W., James, R.H., van Calsteren, P.,
501 Gislason, S.R., and Sigfusson, B. (2008a) The influence of weathering processes
502 on riverine magnesium isotopes in a basaltic terrain. *Earth and Planetary Science*
503 *Letters*, 276(1-2), 187-197.
- 504 Pogge von Strandmann, P.A.E., Elliott, T., Marschall, H.R., Coath, C., Lai, Y.-J.,
505 Jeffcoate, A.B., and Ionov, D.A. (2011) Variations of Li and Mg isotope ratios in
506 bulk chondrites and mantle xenoliths. *Geochimica et Cosmochimica Acta*,
507 75(18), 5247-5268.
- 508 Pogge von Strandmann, P.A.E., James, R.H., van Calsteren, P., Gislason, S.R., and
509 Burton, K.W. (2008b) Lithium, magnesium and uranium isotope behaviour in the
510 estuarine environment of basaltic islands. *Earth and Planetary Science Letters*,
511 274(3-4), 462-471.
- 512 Qiu, Y., Gao, S., McNaughton, N., Groves, D., and Ling, W. (2000) First evidence of
513 > 3.2 Ga continental crust in the Yangtze craton of south China and its
514 implications for Archean crustal evolution and Phanerozoic tectonics. *Geology*,
515 28(1), 11.
- 516 Rudnick, R.L., and Fountain, D.M. (1995) Nature and composition of the continental-
517 crust - a lower crustal perspective. *Reviews of Geophysics*, 33(3), 267-309.
- 518 Rudnick, R.L., and Gao, S. (2003) Composition of the continental crust. In R.L.
519 Rudnick, Ed. *The Crust*, 3, p. 1-64. Elsevier-Pergamon, Oxford.
- 520 Rudnick, R.L., McLennan, S.M., and Taylor, S.R. (1985) Large ion lithophile
521 elements in rocks from high-pressure granulite facies terrains. *Geochimica et*
522 *Cosmochimica Acta*, 49(7), 1645-1655.
- 523 Shen, B., Jacobsen, B., Lee, C.T.A., Yin, Q.Z., and Morton, D.M. (2009) The Mg
524 isotopic systematics of granitoids in continental arcs and implications for the role
525 of chemical weathering in crust formation. *Proceedings of the National Academy*
526 *of Sciences*, 106(49), 20652-20657.
- 527 Teng, F.-Z., Li, W.-Y., Ke, S., Marty, B., Dauphas, N., Huang, S., Wu, F.-Y., and
528 Pourmand, A. (2010a) Magnesium isotopic composition of the Earth and
529 chondrites. *Geochimica et Cosmochimica Acta*, 74(14), 4150-4166.
- 530 Teng, F.-Z., Li, W.-Y., Ke, S., Yang, W., Liu, S.-A., Sedaghatpour, F., Wang, S.-J.,
531 Huang, K.-J., Hu, Y., Ling, M.-X., Xiao, Y., Liu, X.-M., Li, X.-W., Gu, H.-O.,
532 Sio, C.K., Wallace, D.A., Su, B.-X., Zhao, L., Chamberlin, J., Harrington, M.,
533 and Brewer, A. (2015) Magnesium Isotopic Compositions of International

-
- 534 Geological Reference Materials. *Geostandards and Geoanalytical Research*, doi:
535 10.1111/j.1751-908X.2014.00326.x.
- 536 Teng, F.-Z., and Yang, W. (2014) Comparison of factors affecting the accuracy of
537 high-precision magnesium isotope analysis by multi-collector inductively
538 coupled plasma mass spectrometry. *Rapid Communications in Mass
539 Spectrometry*, 28(1), 19-24.
- 540 Teng, F.Z., Li, W.Y., Rudnick, R.L., and Gardner, L.R. (2010b) Contrasting lithium
541 and magnesium isotope fractionation during continental weathering. *Earth and
542 Planetary Science Letters*, 300(1-2), 63-71.
- 543 Teng, F.Z., Rudnick, R.L., McDonough, W.F., Gao, S., Tomascak, P.B., and Liu, Y.S.
544 (2008) Lithium isotopic composition and concentration of the deep continental
545 crust. *Chemical Geology*, 255(1-2), 47-59.
- 546 Teng, F.Z., Wadhwa, M., and Helz, R.T. (2007) Investigation of magnesium isotope
547 fractionation during basalt differentiation: Implications for a chondritic
548 composition of the terrestrial mantle. *Earth and Planetary Science Letters*, 261(1-
549 2), 84-92.
- 550 Teng, F.Z., Yang, W., Rudnick, R.L., and Hu, Y. (2013) Heterogeneous magnesium
551 isotopic composition of the lower continental crust: A xenolith perspective.
552 *Geochemistry Geophysics Geosystems*, 14(9), 3844-3856.
- 553 Tipper, E., Galy, A., and Bickle, M. (2008) Calcium and magnesium isotope
554 systematics in rivers draining the Himalaya-Tibetan-Plateau region: Lithological
555 or fractionation control? *Geochimica et Cosmochimica Acta*, 72(4), 1057-1075.
- 556 Tipper, E.T., Gaillardet, J., Louvat, P., Capmas, F., and White, A.F. (2010) Mg isotope
557 constraints on soil pore-fluid chemistry: Evidence from Santa Cruz, California.
558 *Geochimica et Cosmochimica Acta*, 74(14), 3883-3896.
- 559 Tipper, E.T., Galy, A., and Bickle, M.J. (2006a) Riverine evidence for a fractionated
560 reservoir of Ca and Mg on the continents: Implications for the oceanic Ca cycle.
561 *Earth and Planetary Science Letters*, 247(3-4), 267-279.
- 562 Tipper, E.T., Galy, A., Gaillardet, J., Bickle, M.J., Elderfield, H., and Carder, E.A.
563 (2006b) The magnesium isotope budget of the modern ocean: Constraints from
564 riverine magnesium isotope ratios. *Earth and Planetary Science Letters*, 250(1-2),
565 241-253.
- 566 Wang, S.-J., Teng, F.-Z., and Li, S.-G. (2014a) Tracing carbonate–silicate interaction

-
- 567 during subduction using magnesium and oxygen isotopes. *Nature*
568 *Communications*, 5, doi:10.1038/ncomms6328.
- 569 Wang, S.-J., Teng, F.-Z., Li, S.-G., and Hong, J.-A. (2014b) Magnesium isotopic
570 systematics of mafic rocks during continental subduction. *Geochimica et*
571 *Cosmochimica Acta*, 143(0), 34-48.
- 572 Wang, S.-J., Teng, F.-Z., Williams, H.M., and Li, S.-G. (2012) Magnesium isotopic
573 variations in cratonic eclogites: Origins and implications. *Earth and Planetary*
574 *Science Letters*, 359-360, 219-226.
- 575 Xiao, Y., Teng, F.-Z., Zhang, H.-F., and Yang, W. (2013) Large magnesium isotope
576 fractionation in peridotite xenoliths from eastern North China craton: Product of
577 melt–rock interaction. *Geochimica et Cosmochimica Acta*, 115(0), 241-261.
- 578 Yang, W., Teng, F.-Z., and Zhang, H.-F. (2009) Chondritic magnesium isotopic
579 composition of the terrestrial mantle: A case study of peridotite xenoliths from
580 the North China craton. *Earth and Planetary Science Letters*, 288(3-4), 475-482.
- 581 Yang, W., Teng, F.-Z., Zhang, H.-F., and Li, S.-G. (2012) Magnesium isotopic
582 systematics of continental basalts from the North China craton: Implications for
583 tracing subducted carbonate in the mantle. *Chemical Geology*, 328, 185-194.
- 584 Young, E.D., and Galy, A. (2004) The isotope geochemistry and cosmochemistry of
585 magnesium. In C.M. Hohnson, B.L. Beard, and F. Albarede, Eds. *Geochemistry*
586 *of Non-traditional Stable Isotopes, Reviews in Mineralogy & Geochemistry*, 55,
587 p. 197-230. Mineralogical Society of America, Washington.
- 588 Zhang, H.-F., Zhu, R.-X., Santosh, M., Ying, J.-F., Su, B.-X., and Hu, Y. (2013)
589 Episodic widespread magma underplating beneath the North China Craton in the
590 Phanerozoic: Implications for craton destruction. *Gondwana Research*, 23(1), 95-
591 107.
- 592 Zhou, X., Sun, M., Zhang, G., and Chen, S. (2002) Continental crust and lithospheric
593 mantle interaction beneath North China: isotopic evidence from granulite
594 xenoliths in Hannuoba, Sino-Korean craton. *Lithos*, 62(3-4), 111-124.

595

596 **Table 1**
 597 **Magnesium isotopic compositions of samples from high-grade metamorphic**
 598 **terranes in Eastern China**

Sample	Terrane	n ^a	SiO ₂ ^b	MgO ^b	CIA ^b	δ ⁷ Li ^c	δ ²⁶ Mg	2SD	δ ²⁵ Mg	2SD	Δ ²⁵ Mg ^c
<i>Tonalite gneisses</i>											
D138	Dengfeng	1	62.82	2.62	47	2.8	-0.40	0.06	-0.20	0.04	0.00
D141	Taihau	4	61.38	3.16	41	3.2	-0.35	0.06	-0.16	0.04	0.02
14R109	Wutai	10	62.67	2.63	50	5.2	-0.22	0.06	-0.11	0.04	0.00
14R110	Wutai	10	70.84	1.89	52	2.6	0.12	0.06	0.06	0.04	0.00
14R118	Wutai	15	61.03	2.89	47	5.6	-0.31	0.06	-0.13	0.04	0.03
14R117	Wutai	15	61.34	2.58	48	5.2	-0.23	0.06	-0.13	0.04	-0.01
<i>Trondhjemite gneisses</i>											
14R116	Wutai	15	69.32	1.04	51	7.5	-0.30	0.06	-0.17	0.04	-0.01
D142	Taihau	1	72.54	0.40	51	3.9	-0.29	0.09	-0.17	0.07	-0.02
D139	Dengfeng	3	72.39	0.60	54	3.7	-0.31	0.09	-0.18	0.07	-0.02
D147	Kongling	7	67.60	2.08	49	2.9	-0.24	0.09	-0.13	0.07	-0.01
<i>Granite gneisses</i>											
D143	Taihau	3	72.03	0.58	50	4.0	-0.35	0.09	-0.18	0.07	-0.01
D140	Dengfeng	2	72.32	0.46	51	3.8	-0.24	0.09	-0.11	0.07	0.01
D148	Kongling	4	71.84	1.31	53	2.7	-0.05	0.09	-0.02	0.07	0.00
<i>Amphibolites</i>											
D149	Dengfeng	10	51.41	6.09	41	3.4	-0.20	0.09	-0.10	0.07	0.00
D153	Taihau	12	50.81	5.76	39	6.8	-0.25	0.09	-0.09	0.07	0.04
14R162	Fuping	2	47.05	7.73	38	3.9	-0.17	0.09	-0.07	0.07	0.02
14R167	Hengshan	8	50.71	5.71	40	3.7	-0.22	0.07	-0.14	0.05	-0.03
D171	Kongling	8	49.54	6.84	38	6.2	-0.26	0.07	-0.11	0.05	0.02
<i>Mafic granulites</i>											
D154	Taihau	2	50.08	5.91	38	4.4	-0.19	0.07	-0.09	0.05	0.01
14R161	Fuping	8	50.71	5.17	35	4.7	-0.16	0.07	-0.06	0.05	0.02
14R168	Hengshan	1	48.86	4.51	33	5.7	-0.20	0.07	-0.09	0.05	0.02
D368	Jinning	10	45.69	6.54	38	3.4	-0.16	0.07	-0.08	0.05	0.01
<i>Intermediate granulites</i>											
15R281	Wulashan	10	54.54	4.52	41	2.3	-0.21	0.07	-0.08	0.05	0.03
15R267	Wulashan	10	61.60	3.54	45	5.1	-0.22	0.07	-0.12	0.05	0.00
15R278	Wulashan	10	62.33	2.38	45	3.2	-0.21	0.07	-0.11	0.05	0.00
15R266	Wulashan	10	62.76	1.55	47	2.4	-0.17	0.07	-0.07	0.04	0.02
<i>Felsic granulites</i>											
D366	Jinning	3	59.00	3.07	47	2.8	-0.19	0.07	-0.11	0.04	-0.01
15R277	Wulashan	10	65.27	2.11	47	1.7	-0.19	0.07	-0.10	0.04	0.00
15R268	Wulashan	10	65.53	1.69	47	3.1	-0.15	0.07	-0.08	0.04	-0.01
15R263	Wulashan	10	70.36	0.66	50	2.8	-0.17	0.07	-0.12	0.04	-0.03

599 ^a n = number of individual samples comprising the composite.

600 ^b Data from Gao et al. (1998a), CIA = Chemical Indexes of Alteration, defined as = molecular
 601 ratios of Al₂O₃/(Al₂O₃ + CaO + Na₂O + K₂O) × 100 (Nesbitt and Young, 1982)..

602 ^c Data from Teng et al. (2008).

603 **Table 2**

604 **Magnesium isotopic compositions of the Hannuoba granulite xenoliths**

Sample	SiO ₂ ^a	MgO ^a	Mg# ^a	δ ⁷ Li ^b	δ ²⁶ Mg	2SD	δ ²⁵ Mg	2SD	Δ ²⁵ Mg'
<i>Pyroxenite</i>									
DMP-10	48.99	18.62	76	-4.2	-0.30	0.07	-0.18	0.04	-0.03
<i>Two-pyroxene mafic granulites</i>									
DMP-03	49.07	14.01	79	0.5	-0.35	0.07	-0.16	0.04	0.02
DMP-09	49.54	18.37	78	-1.9	-0.35	0.07	-0.20	0.04	-0.02
DMP-11	49.83	20.18	77	-1.9	-0.28	0.07	-0.15	0.04	0.00
DMP-28	50.30	13.85	70	-8.0	-0.26	0.03	-0.11	0.03	0.02
DMP-45	50.66	15.06	74	-9.6	-0.33	0.03	-0.14	0.03	0.02
DMP-66	50.51	13.58	78	-2.9	-0.30	0.03	-0.15	0.03	0.00
DMP-68	49.74	16.23	78	-3.3	-0.27	0.03	-0.11	0.03	0.03
<i>Garnet-bearing mafic granulites</i>									
DMP-08	45.27	12.42	72	0.2	-0.37	0.03	-0.18	0.03	0.01
DMP-15	44.21	14.69	70	4.3	-0.31	0.03	-0.16	0.03	0.00
<i>Plagioclase-rich mafic granulites</i>									
DMP-06	51.72	6.97	64	13.8	-0.65	0.03	-0.34	0.03	-0.01
DMP-07	45.71	5.07	61	2.2	-0.67	0.07	-0.34	0.05	0.00
DMP-62	52.92	5.81	72	6.7	-0.74	0.07	-0.38	0.05	0.00
DMP-75	52.43	5.18	56	1.3	-0.42	0.07	-0.21	0.05	0.00
<i>Intermediate granulites</i>									
DMP-01	60.30	4.96	72	12.1	-0.44	0.07	-0.23	0.05	-0.01
DMP-27	54.00	3.74	47	-5.1	-0.24	0.07	-0.12	0.05	0.00
DMP-61	57.48	2.95	70	3.8	-0.76	0.07	-0.39	0.05	0.00
DMP-70	56.82	5.34	65	7.1	-0.56	0.07	-0.29	0.05	-0.01

605

606 ^a Data from Liu et al. (2001).

607 ^b Data from Teng et al. (2008).

608

609

610 **Figure captions:**

611 Figure 1. Cratons of eastern China with composite sampling area (dashed line box)
612 and the Hannuoba granulite xenoliths (black circle) outlined. Numbers 1 to 8
613 correspond to the eight Archean terranes.

614 Figure 2. (a) MgO vs. SiO₂, (b) $\delta^7\text{Li}$ vs. SiO₂ for the high-grade metamorphic terrane
615 composites and the Hannuoba granulite xenoliths. Database: MgO and SiO₂ for
616 the high-grade metamorphic terrane composites and the Hannuoba granulite
617 xenoliths are from Gao et al. (1998a) and Liu et al. (2001), respectively. Lithium
618 isotopic data are from Teng et al. (2008).

619 Figure 3. P-T estimates for the Hannuoba granulite xenoliths and experimentally
620 constrained equilibria of decarbonation of carbonated basalts (modified from
621 (Dasgupta, 2013). Under the P-T condition of the Hannuoba granulite xenoliths,
622 they will experience complete decarbonation, which is consistent with the
623 observation that carbonate mineral is absent in these rocks.

624 Figure 4. Magnesium three-isotope plot of the samples in this study. The solid line
625 represents the equilibrium mass fractionation line with a slope equal to 0.521.
626 Error bars represent 2SD uncertainties. Data are from Tables 1 and 2.

627 Figure 5. $\delta^{26}\text{Mg}$ vs. MgO (wt%) for the high-grade metamorphic terrane composites
628 and the Hannuoba granulite xenoliths. The grey bar represents the average
629 mantle ($\delta^{26}\text{Mg} = -0.25 \pm 0.07$) (Teng et al., 2010a). Error bars represent 2SD
630 uncertainties. Data are from Tables 1 and 2.

631 Figure 6. (a) $\delta^{26}\text{Mg}$ vs. rock type, (b) $\delta^{26}\text{Mg}$ vs. sample locality for the high-grade
632 metamorphic terrane composites. T = Tonalite gneiss, TR = Trondhjemite gneiss,
633 G = Granite gneiss, A = Amphibolite, M = Mafic granulite, I = Intermediate
634 granulite, F = Felsic granulite. The grey bar represents the average mantle
635 ($\delta^{26}\text{Mg} = -0.25 \pm 0.07$) (Teng et al., 2010a). Error bars represent 2SD

636 uncertainties. Data are from Table 1.

637 Figure 7. (a) $\delta^{26}\text{Mg}$ vs. Cr/Ho, (b) $\delta^{26}\text{Mg}$ vs. Ni/Ho for the Hannuoba high Mg
638 granulite xenoliths. Database: Cr/Ho and Ni/Ho are from Liu et al. (2001), $\delta^{26}\text{Mg}$
639 from Table 2, the two samples with preferential sampling of garnet from Teng et
640 al. (2013). Error bars represent 2SD uncertainties.

641 Figure 8. (a) $\delta^{26}\text{Mg}$ vs. $^{206}\text{Pb}/^{204}\text{Pb}$, (b) $\delta^{26}\text{Mg}$ vs. $\epsilon_{\text{Nd}}(t)$ for the Hannuoba granulite
642 xenoliths. Database: $^{206}\text{Pb}/^{204}\text{Pb}$ and $\epsilon_{\text{Nd}}(t)$ from Liu et al. (2004) and $\delta^{26}\text{Mg}$ from
643 Table 3. Error bars represent 2SD uncertainties. The grey bar represents mixing
644 between preexisting Precambrian deep crust with the underplated basalts. If the
645 mixing is the major mechanism to generate the large Mg isotopic variation in the
646 Hannuoba granulite xenoliths, the underplated basalt should have a very light Mg
647 isotopic composition ($\delta^{26}\text{Mg} < -0.76\text{‰}$).

648 Figure 9. $\delta^{26}\text{Mg}$ vs. $\delta^7\text{Li}$ for the high-grade metamorphic terrane composites and the
649 Hannuoba granulite xenoliths. Database: $\delta^7\text{Li}$ from Teng et al. (2008) and $\delta^{26}\text{Mg}$
650 from Tables 1 and 2. Error bars represent 2SD uncertainties.

651 Figure 10. (a) $\delta^{26}\text{Mg}$ vs. H_2O , (b) Rb vs. H_2O , (c) Ba vs. H_2O for the Hannuoba
652 granulite xenoliths. Database: H_2O , Rb and Ba from Liu et al. (2001) and $\delta^{26}\text{Mg}$
653 from Table 2. Error bars represent 2SD uncertainties.

654 Figure 11. Magnesium isotopic composition of the crustal samples. Database: $\delta^{26}\text{Mg}$
655 data of upper crustal rocks are from Li et al. (2010), Liu et al. (2010), Ling et al.
656 (2013) and Huang et al. (2013a); Middle crustal rocks are from Table 1; Lower
657 crustal rocks are from Teng et al. (2013) and Table 2. The gray bar represents the
658 average mantle ($\delta^{26}\text{Mg} = -0.25 \pm 0.07$) (Teng et al., 2010a).

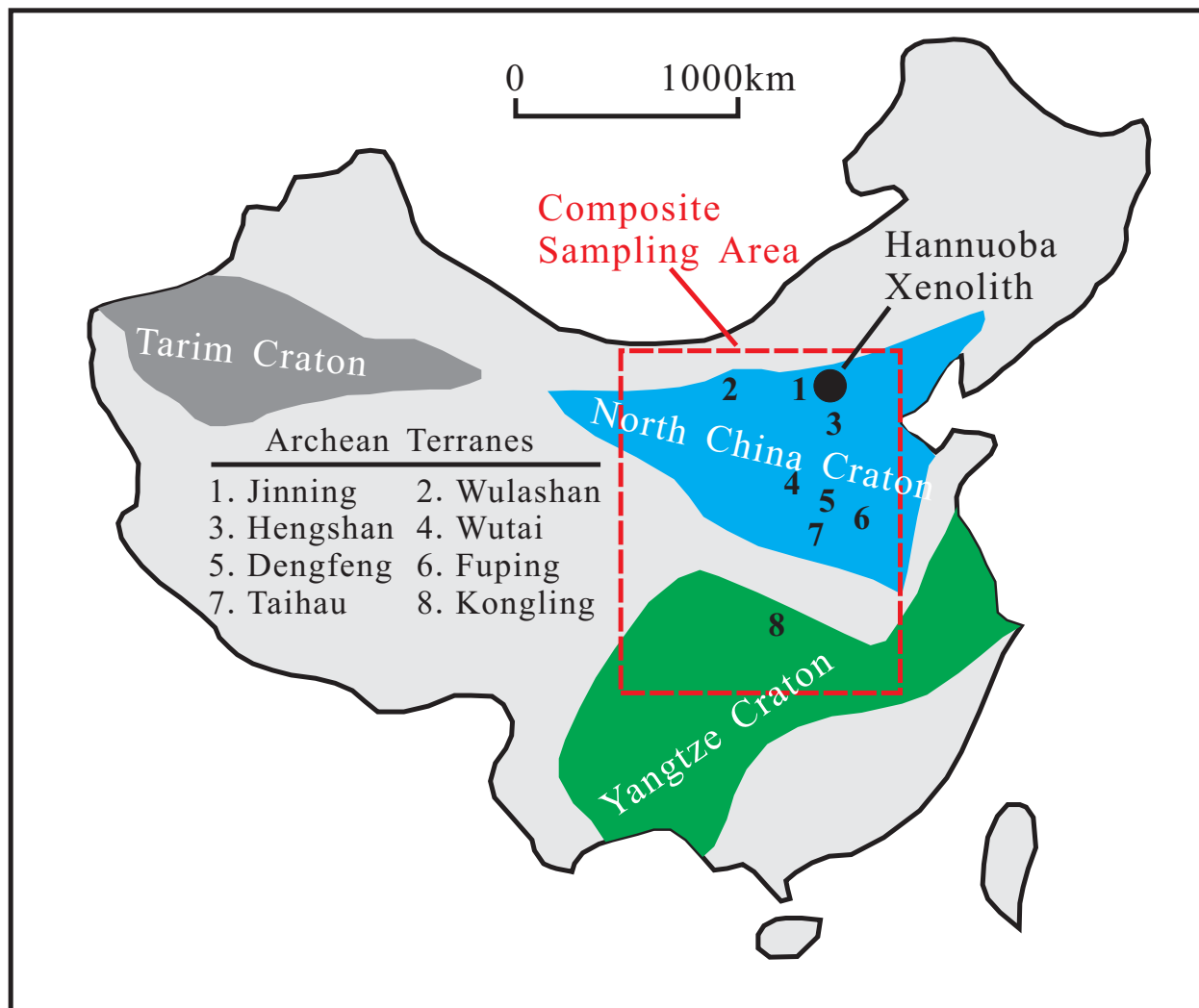


Figure 1

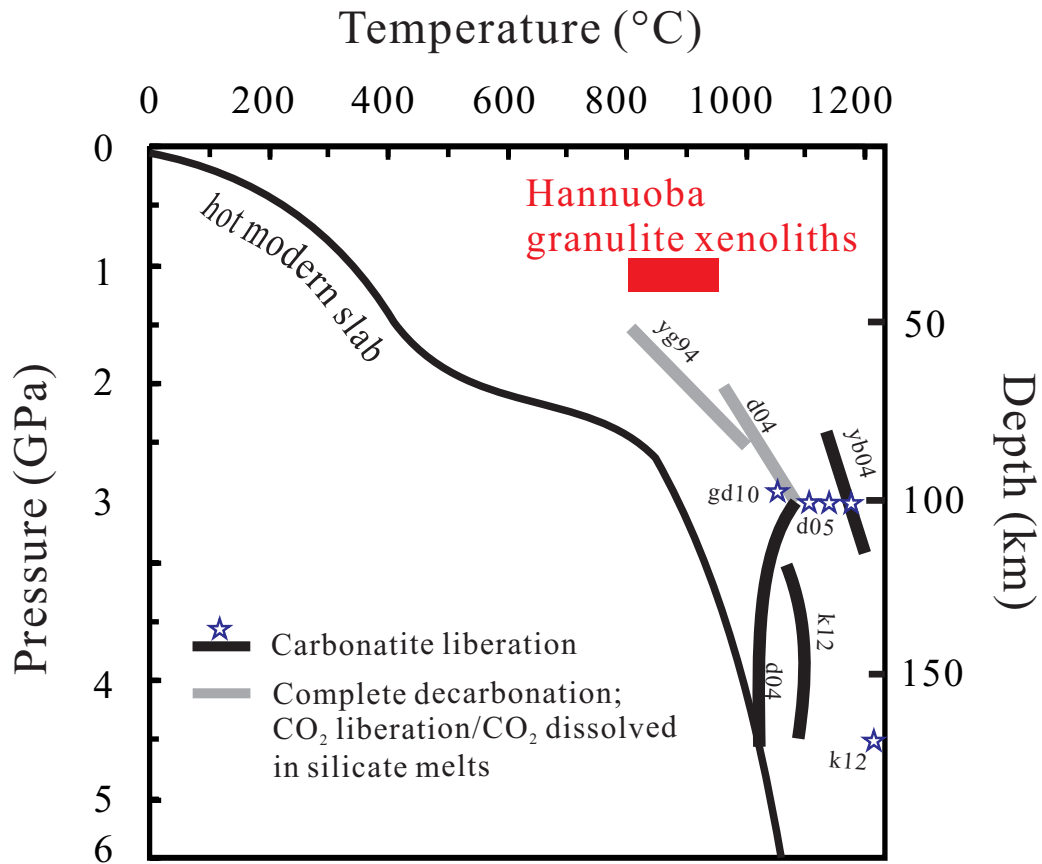


Figure 3

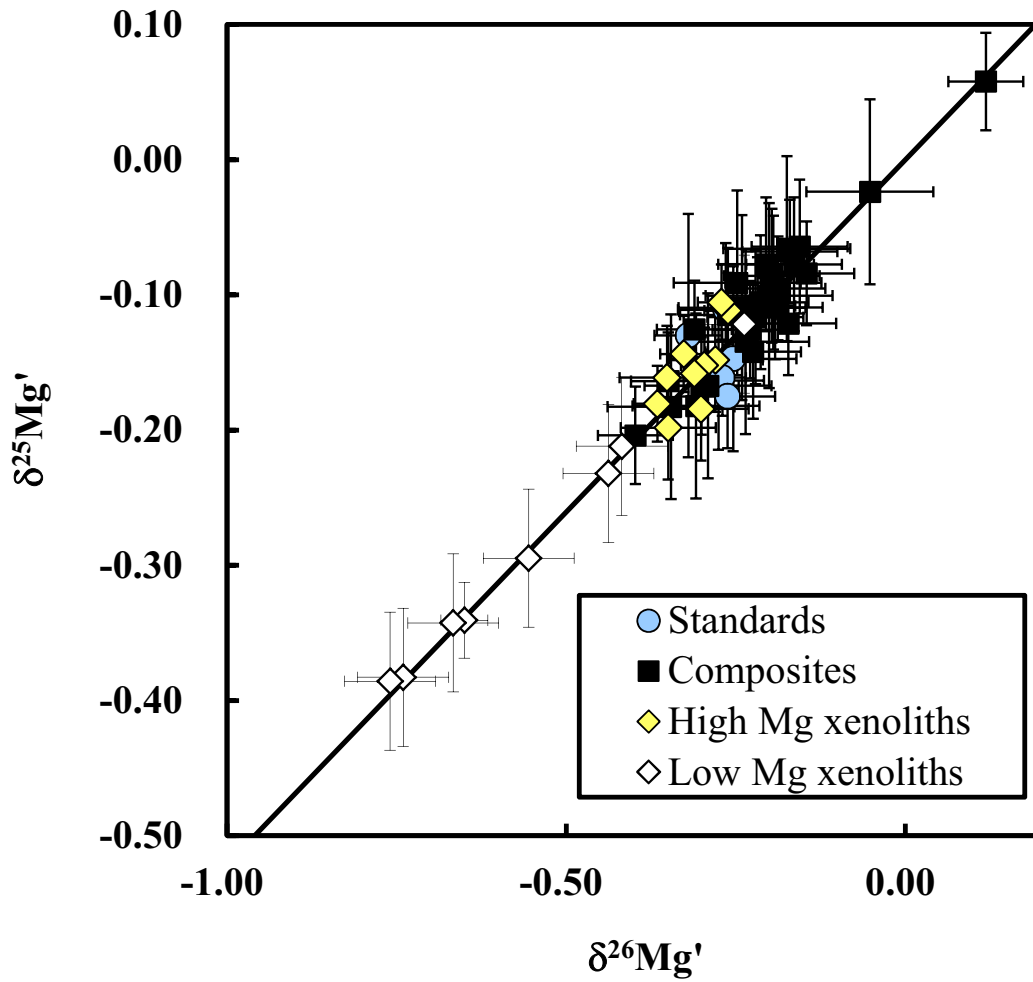


Figure 4

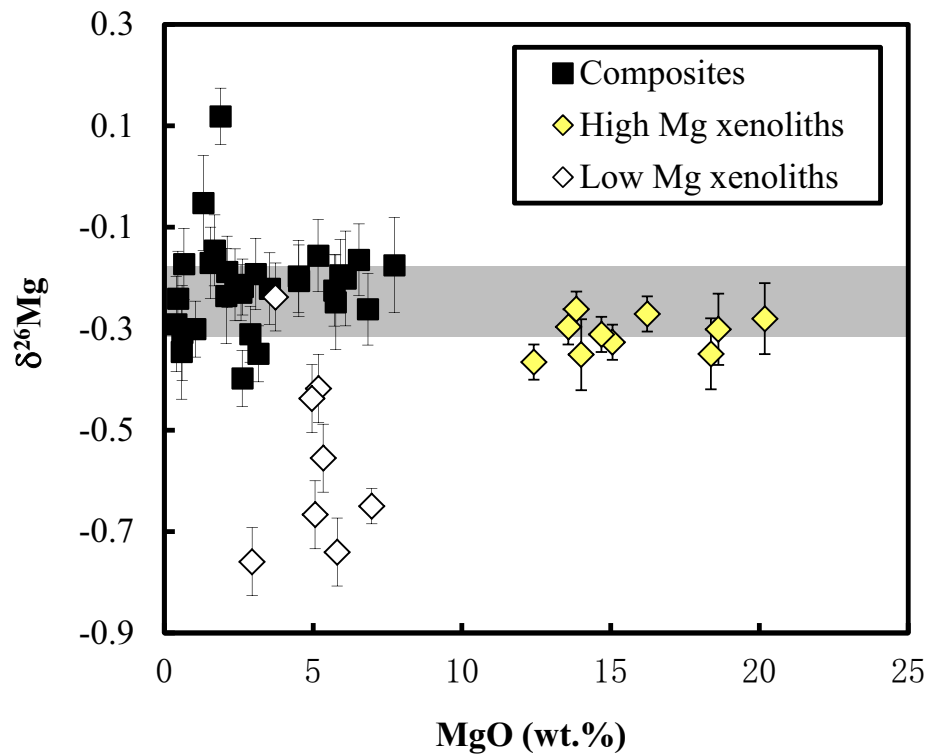


Figure 5

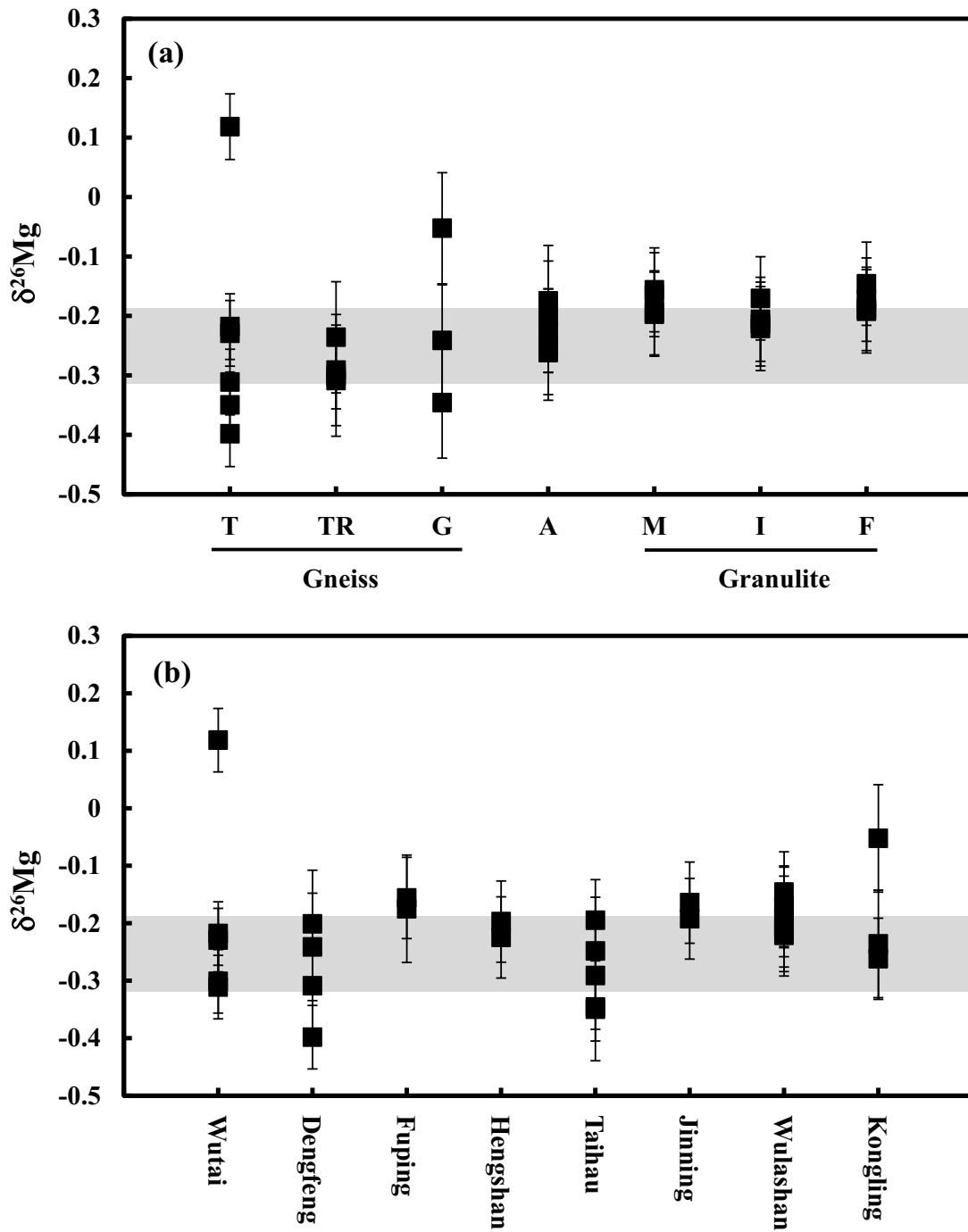


Figure 6

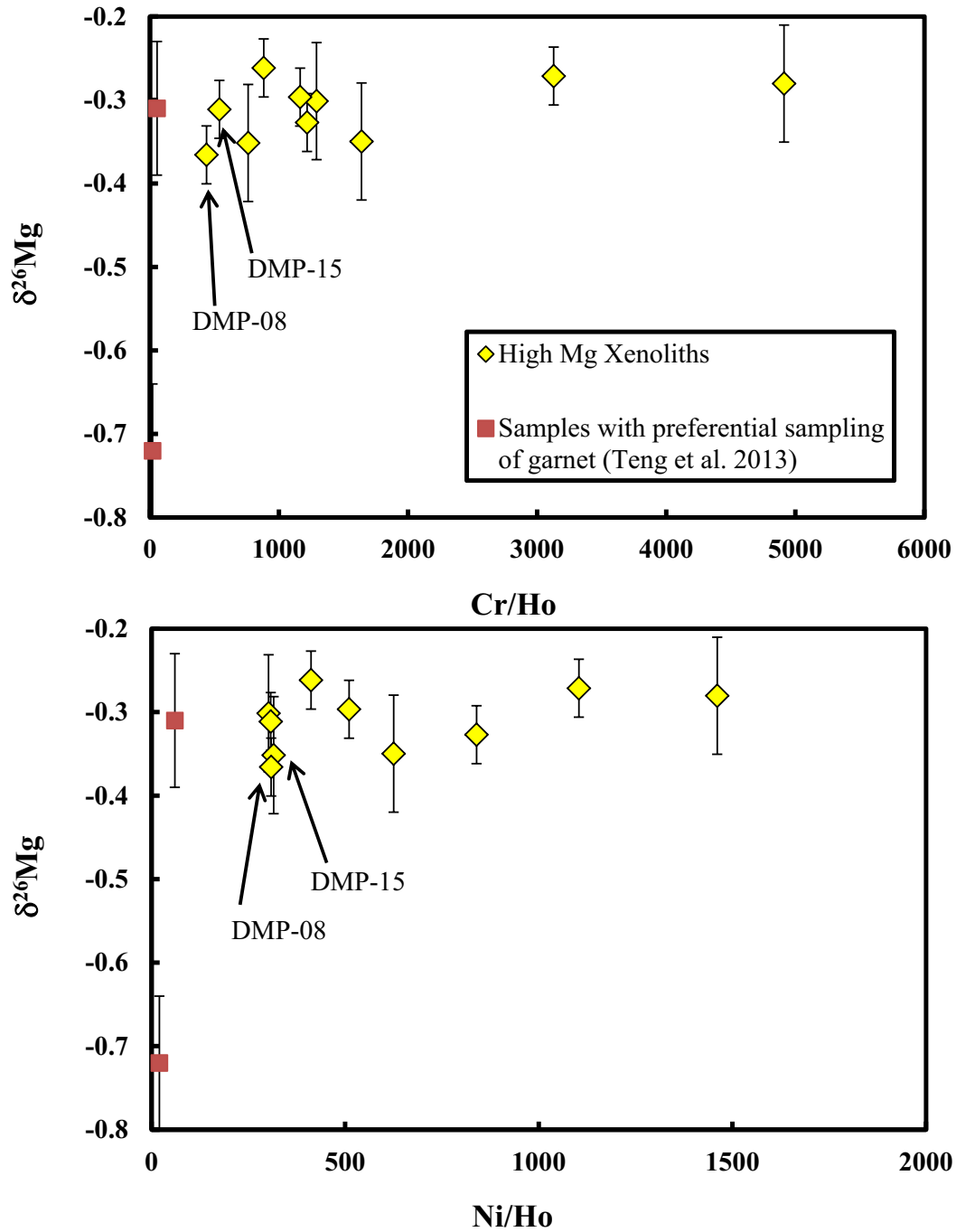


Figure 7

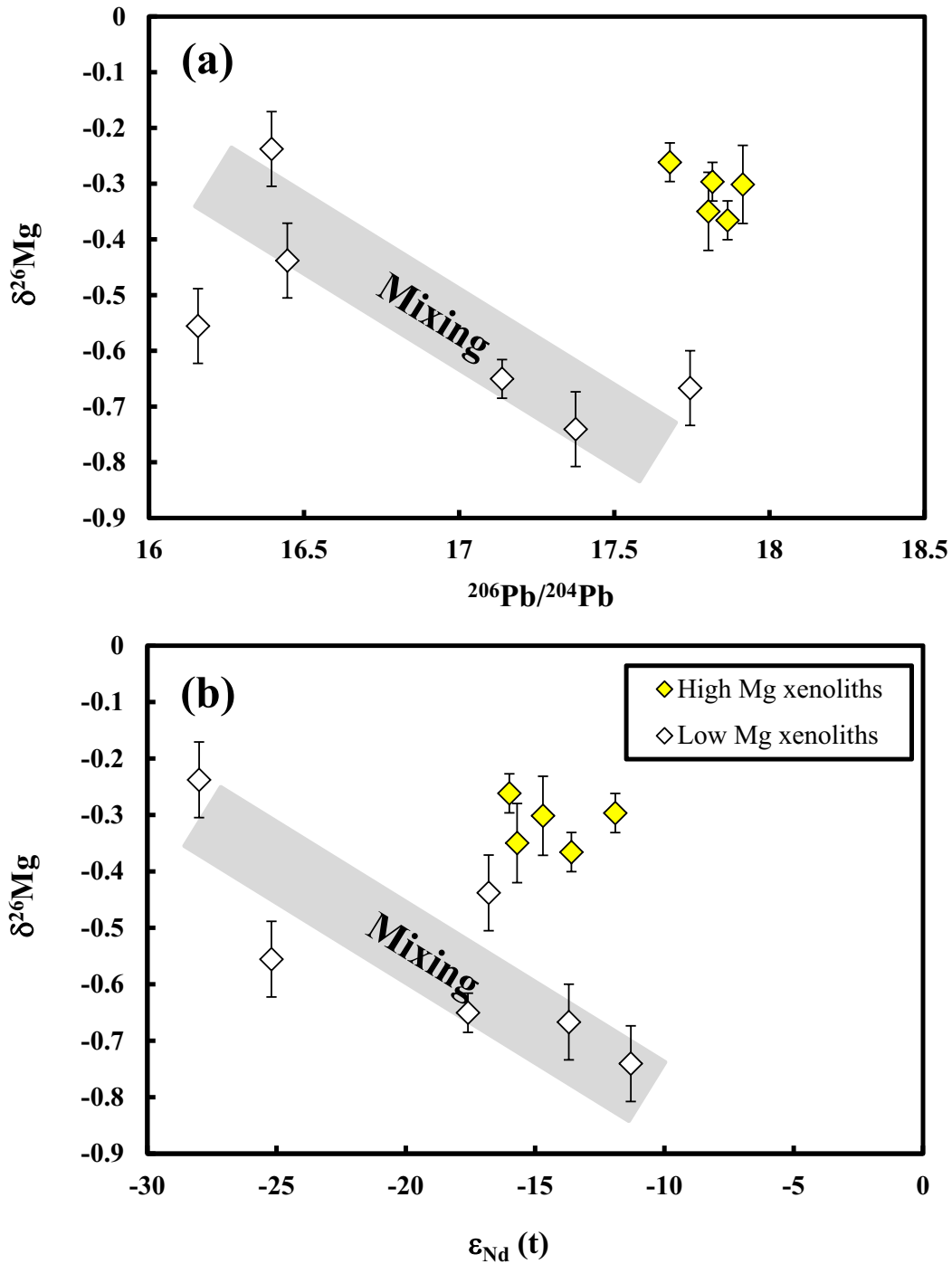


Figure 8

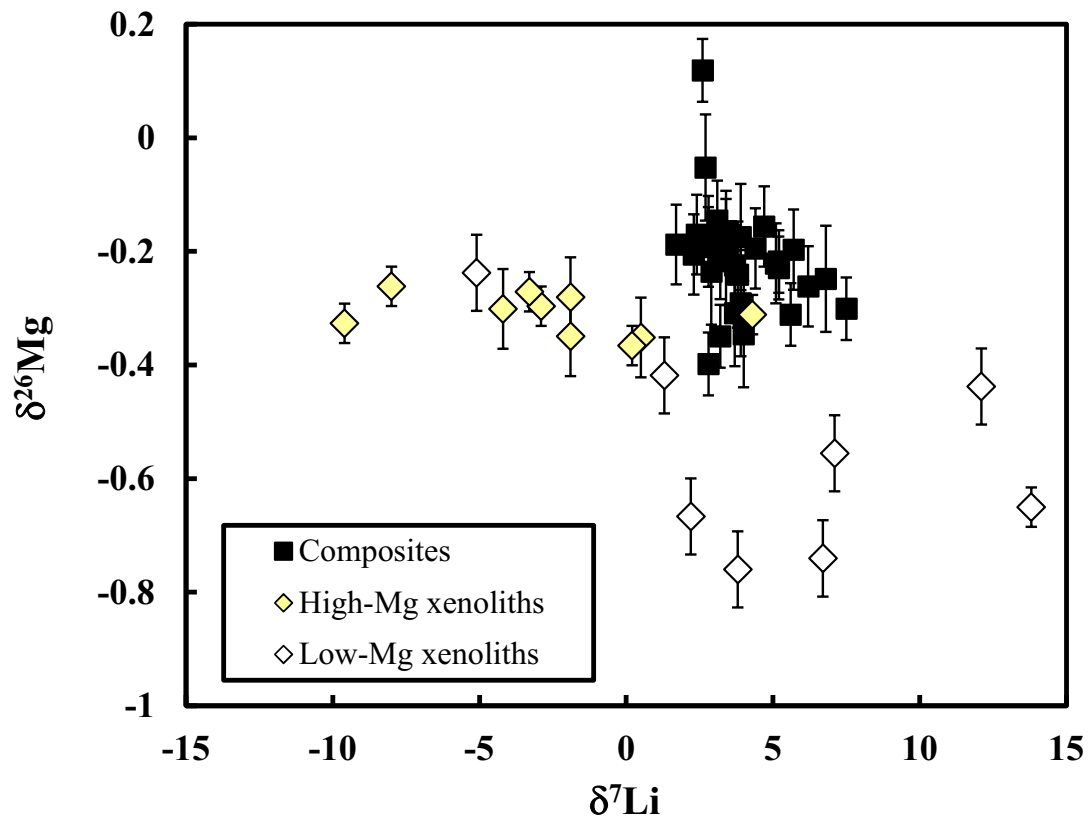


Figure 9

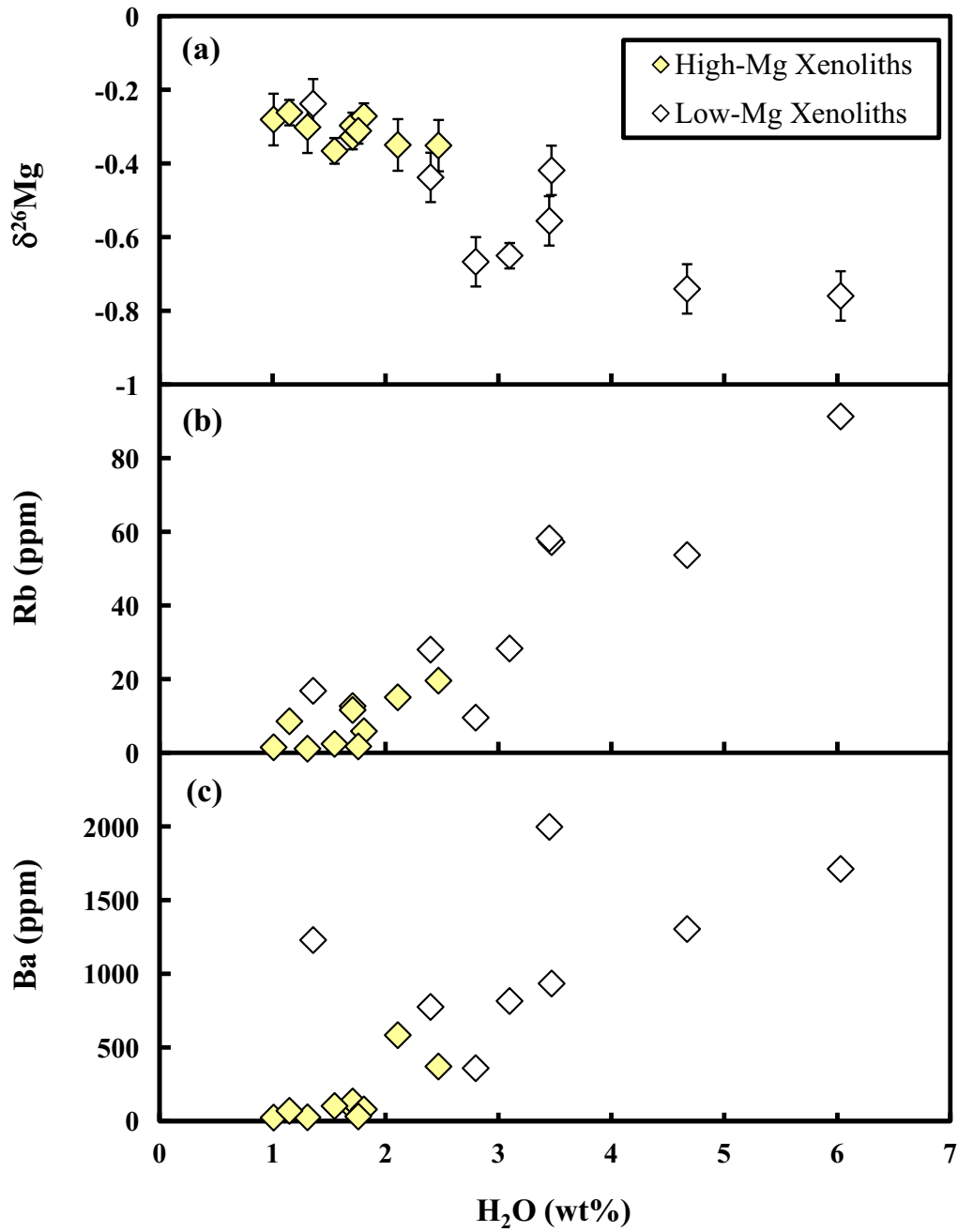


Figure 10

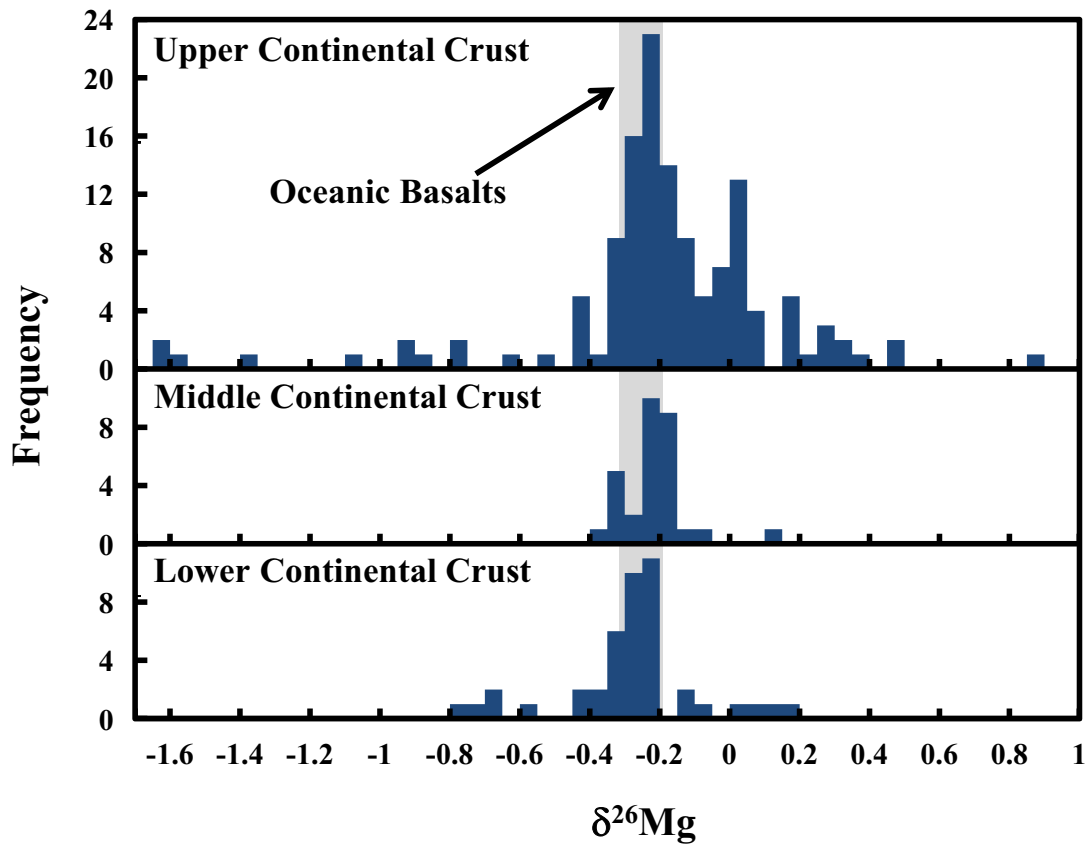


Figure 11